

Near-infrared/optical identification of five low-luminosity X-ray pulsators^{*}

Ramanpreet Kaur^{1,†}, Rudy Wijnands¹, Biswajit Paul², Alessandro Patrino¹,
Nathalie Degenaar¹

¹ *Astronomical Institute "Anton Pannekoek", University of Amsterdam, Science Park 904, 1098 XH, Amsterdam, The Netherlands*

² *Raman Research Institute, C. V. Raman Avenue, Sadashivanagar, Bangalore 560 080, India.*

1 November 2018

ABSTRACT

We present the identification of the most likely near-infrared/optical counterparts of five low-luminosity X-ray pulsators (AX J1700.1–4157, AX J1740.1–2847, AX J1749.2–2725, AX J1820.5–1434 and AX J1832.3–0840) which have long pulse periods (> 150 s). The X-ray properties of these systems suggest that they are likely members of persistent high mass X-ray binaries or intermediate polars. Using our *Chandra* observations, we detected the most likely counterparts of three sources (excluding AX J1820.5–1434 and AX J1832.3–0840) in their ESO - NTT near-infrared observations, and a possible counterpart for AX J1820.5–1434 and AX J1832.3–0840 in the 2MASS and DSS observations respectively. We also performed the X-ray timing and spectral analysis for all the sources using our *XMM-Newton* observations, which further helped us to constrain the nature of these systems. Our multiwavelength observations suggest that AX J1749.2–2725 and AX J1820.5–1434 most likely harbor accreting neutron stars while AX J1700.1–4157, AX J1740.1–2847 and AX J1832.3–0840 could be intermediate polars.

Key words: binaries: close - pulsars: low-luminosity pulsars: individual (AX J1700.1–4157, AX J1740.1–2847, AX J1749.2–2725, AX J1820.5–1434, AX J1832.3–0840) - stars: neutron - X-rays: binaries: supernova

1 INTRODUCTION

During the last decade, a number of Galactic sub-luminous X-ray pulsators ($L_X \sim 10^{34} - 10^{35}$ erg s⁻¹) have been discovered with pulse periods ranging from a few seconds to over a thousand seconds. Most of these pulsators are discovered during Galactic plane surveys performed using various X-ray telescopes, e.g., *BeppoSAX*, *ASCA*, and *RXTE*, and are found to harbor a variety of source-types like anomalous X-ray pulsars (isolated slowly rotating neutron stars; e.g., Torii et al. 1998), accreting magnetized white dwarfs (i.e., intermediate polars (IPs); e.g., Misaki et al. 1996) and neutron stars accreting from high mass companions (i.e., mostly Be/X-ray binaries; e.g., Hulleman et al. 1998). A majority of these systems are transient in nature, but there are several persistent systems also emitting at such low-luminosities. Among these persistent systems, there remains a group of

sources whose nature has not been determined yet. The X-ray properties of most of these persistent systems suggest that they could be neutron stars accreting from a high mass star or accreting white dwarf systems. Furthermore, in some cases, the possibility of a system in which a neutron star accretes from a low mass star also cannot be excluded (Lin et al. 2002).

Most of the known Be/X-ray binaries are transient in nature and this behaviour is usually associated with their highly eccentric orbits (Okazaki and Negueruela 2001). A sub-class of Be/X-ray binaries characterized by persistent, low-luminosity X-ray emission, and slowly rotating pulsars, has recently been proposed by Reig and Roche (1999). The neutron star in these systems is assumed to be orbiting its companion Be star in a relatively wide and a circular orbit, hence accreting from the low-density outer regions of the circumstellar envelope. Pfahl et al. (2002) has proposed a possible scenario for the formation of these wide orbit (> 30 days) and low-eccentricity (< 0.2) high mass X-ray binaries, suggesting that these systems could have formed in

^{*} Based on observations obtained from ESO Science Archive Facility under programs 66.D-0440(B) and 69.D-0339(A)

[†] E-mail: r.kaur@uva.nl

a supernova explosion, accompanied with a very small kick ($\lesssim 50$ km/s) to the neutron star. If true, this growing class of persistent Be/X-ray binaries would help us to explore a different type of supernova explosion.

This paper is a part of our ongoing project to find the true nature of low-luminosity X-ray pulsators. In our previous paper, we reported the identification of NIR counterparts of two low-luminosity X-ray pulsators - SAX J1324.4-6200 and SAX J1452.8-4959 using the *Chandra* and the *XMM-Newton* observations (Kaur et al. 2009). It was suggested that SAX J1324.4-6200 is likely a HMXB pulsar while no firm conclusion about the nature of SAX J1452.8-4959 could be drawn. In this paper, we report on the identification of the most likely counterparts of additional five low-luminosity X-ray pulsators - AX J1700.1-4157, AX J1740.1-2847, AX J1749.2-2725, AX J1820.5-1434 and AX J1832.3-0840. These sources were discovered from the Galactic plane observations made in 1995 - 1999 using the *ASCA* satellite (Sugizaki et al. 2001). The basic physical parameters with which these sources were discovered are listed in Table 1.

2 X-RAY OBSERVATIONS

We carried out X-ray observations of the five X-ray pulsators listed in Table 1 using the European Photon Imaging Camera (EPIC) aboard the *XMM-Newton* satellite and the Advanced CCD Imaging Spectrometer (ACIS) aboard the *Chandra* satellite.

2.1 *XMM-Newton*

The X-ray pulsators were observed for 7 - 32 ks each using the EPIC instruments on the *XMM-Newton* satellite. The observation details are summarized in Table 2. During our observations, both the EPIC-*MOS* and *pn* cameras (Turner et al. 2001; Strüder et al. 2001) were operated in the *Full Frame* mode and with the medium filter. The EPIC data was processed using the *XMM-Newton* Science Analysis System (SAS version 7.1.0)¹.

Investigation of the full-field count-rate of X-ray pulsators revealed no high-count rate background particle flaring in all of them so all data could be used. During our observations for all the targets, we detected only one source inside the error circle from the *ASCA* observations. The detection of pulsations in all of them (see Section 3) further confirmed their identity. We used the task *edetect_chain* to find the exact position of the X-ray sources (see Table 2) in their combined EPIC-*MOS* and *pn* image. The error circle on the position of each X-ray source is adopted as a quadratic sum of the bore sight error of the *XMM-Newton* telescope² and the statistical error given by the task *edetect_chain* and is $\sim 2''.0$ for all the targets.

2.2 *Chandra*

The X-ray pulsators were observed for ~ 1 ks each using the ACIS-I instrument on the *Chandra* satellite in the

FAINT mode. The details of these observations are summarized in Table 2. We processed the ACIS-I event 2 files using the standard software packages CIAO 4.0³ and CALDB 3.4.2⁴. The task *wavdetect* was used to find the exact position of the targets in the ACIS-I images and are listed in Table 2. The error circle on the position is adopted as a quadratic sum of the bore sight error of the *Chandra* telescope⁵ ($0''.6$, Aldcroft et al. 2000), $1\text{-}\sigma$ *wavdetect* errors and a contribution that depends on the number of detected counts (van den Berg et al. 2004) and is found to be $\sim 0''.64$ for all the sources.

3 X-RAY TIMING ANALYSIS

The *XMM-Newton* EPIC-*MOS* and *pn* observations are used for the timing analysis of our targets. The X-ray events were extracted in a circular region of radius $30''$ centered on the position of the X-ray source in their EPIC-*MOS* and *pn* images, with a time resolution of 0.1 s. Similarly, the background X-ray events were extracted for each source from a source-free region on the same CCD. The event times were then transformed to barycentric times using the *Chandra* position of the X-ray source and the JPL-DE405 ephemeris using the task *barycor* in *SAS*. The background was subtracted to generate the background corrected light curves separately for EPIC-*MOS* and *pn* instruments, which were then added to generate the final lightcurves for our timing analysis.

We searched for the spin-period in the lightcurves using the task *powspec* in *FTOOLS*⁶ and refined it further using the task *efsearch*. The pulse periods thus detected for all pulsators are listed in Table 3 except for AX J1820.5-1434. We phase connected the pulsations for AX J1820.5-1434, using EPIC - *pn* observations, by cross-correlating each single profile with a standard profile obtained by folding the entire data set. This method gave us a pulse period of AX J1820.5-1434 with a much better accuracy, $P_s = 153.24 \pm 0.02$ s (listed in Table 3). The errors on the pulse periods are calculated at the 68% confidence level. Given the short-baseline of all the observations, it was not possible to measure the spin period derivative (\dot{P}) for all the sources with a phase coherent technique. However, we fitted the previous (see Table 1) and the new measured values of the spin-period (see Table 3) with a linear relation and determined the spin-period derivative of AX J1820.5-1434 to be $(3.00 \pm 0.14) \times 10^{-9}$ s s⁻¹ and an upper limit for the remaining sources (see Table 3). Assuming an orbital velocity of the pulsating component to be ~ 300 km s⁻¹, the difference in pulse period (ΔP_s) measured in different orbital phases would be $\sim P_s/1000$. However, in case of AX J1820.5-1434, the measured ΔP_s is 0.98 s ($\sim P_s/100$), indicates that the measured period derivative is significantly more than that caused by the orbital motion.

The obtained X-ray lightcurves are folded in one single

³ *Chandra* Interactive Analysis of Observations (CIAO), <http://cxc.harvard.edu/ciao/>.

⁴ *Chandra* Calibration Database (CALDB), <http://cxc.harvard.edu/caldb/>

⁵ see <http://cxc.harvard.edu/cal/ASPECT/celmon>.

⁶ <http://heasarc.gsfc.nasa.gov/docs/software/ftools/ftools.menu.html>

¹ see <http://xmm2.esac.esa.int/sas/>

² see <http://xmm2.esac.esa.int/docs/documents/CAL-TN-0018.pdf>

Table 1. Summary of basic parameters of our sample of X-ray pulsators.

Object	l	b	Spin period (in seconds)	Absorbed flux ($\times 10^{-12}$ erg cm $^{-2}$ s $^{-1}$) (2 - 10 keV)	Spectral parameters		References
					N_{H} ($\times 10^{22}$ cm $^{-2}$)	Γ	
AX J1700.1–4157	344.04	0.24	714.5 ± 0.3	6	6	0.7	1
AX J1740.1–2847	359.49	1.09	729 ± 14	4	3	0.7	2
AX J1749.2–2725	1.70	0.11	220.38 ± 0.20	3 - 30	10	1.0	3
AX J1820.5–1434	16.47	0.07	152.26 ± 0.04	23	10	0.9	4
AX J1832.3–0840	23.04	0.26	1549.1 ± 0.4	11	1	0.8	5

REFERENCES. – (1) Torii et al. 1999 (2) Sakano et al. 2000 (3) Torii et al. 1998 (4) Kinugasa et al. 1998 (5) Sugizaki et al. 2000

 NOTE : In this table, l and b represent the Galactic longitude and latitude of a given star respectively. The spectral parameters, N_{H} and Γ , represent the neutral hydrogen column density and the power-law index respectively.

Table 2. X-ray observation details.

Object	Telescope	Date (UT)	ObsId	Duration (ks)	R.A.	DEC.
					hh:mm:ss	° ' "
AX J1700.1–4157	<i>XMM-Newton</i>	17 Feb 2008	0511010601	7.9	17:00:04.32	–41:58:04.44
	<i>Chandra</i>	30 Jun 2008	9015	1.13	17:00:04.35	–41:58:05.46
AX J1740.1–2847	<i>XMM-Newton</i>	27 Feb 2008	0511010701	9.3	17:40:09.12	–28:47:26.16
	<i>Chandra</i>	06 Sep 2008	9016	1.17	17:40:09.12	–28:47:26.02
AX J1749.2–2725	<i>XMM-Newton</i>	04 Mar 2008	0511010301	8.9	17:49:12.24	–27:25:37.56
	<i>Chandra</i>	27 Apr 2008	9013	1.18	17:49:12.41	–27:25:38.21
AX J1820.5–1434	<i>XMM-Newton</i>	30 Sep 2007	0511010101	11.2	18:20:30.00	–14:34:23.16
	<i>Chandra</i>	03 Sep 2008	9011	1.15	18:20:30.09	–14:34:23.52
AX J1832.3–0840	<i>XMM-Newton</i>	16 Oct 2007	0511010801	31.3	18:32:19.44	–08:40:30.47
	<i>Chandra</i>	07 Aug 2008	9017	1.16	18:32:19.30	–08:40:30.44

 NOTE : The error circle on the *Chandra* and the *XMM-Newton* observations is $\sim 0''.64$ and $\sim 2''.0$ respectively for all the sources.

profile to measure the pulse fractional amplitude defined as $(F_{\text{max}} - F_{\text{min}})/(F_{\text{max}} + F_{\text{min}})$ where F_{max} and F_{min} are the maximum and minimum flux (or counts) in a pulse profile. The pulse profiles of all the sources thus obtained are shown together in Figure 1 where the pulse profile of SAX J1324.4–6200 is taken from Kaur et al. (2009) for comparison. Out of the six sources listed in Table 3, four sources clearly showed single peak profiles, while AX J1740.1–2847 and AX J1832.3–0840 showed double peak profiles.

4 X-RAY SPECTRAL ANALYSIS

Using the *XMM-Newton* data, we also performed spectral analysis of our targets. We used the same extraction region for both these instruments as were used for the timing analysis reported in Section 3. The SAS tool *xmmselect* was used to extract both the source and the background spectra and *XSPEC* (version 12.0.0) was used for the spectral fitting. The resulting spectra were re-binned to have minimum of 20 counts per bin.

We fitted a variety of single component models to the spectra. The X-ray spectra of most of our sources could be fitted well using the absorbed power-law and the blackbody models. For all pulsators, the values of the measured fit parameters using these two models are given in Table 4. The absorbed as well as the unabsorbed fluxes for the fitted models in 2 - 10 keV energy band are also given in the same table. Figure 2 shows the best fit powerlaw model to the

X-ray spectra of our targets, except for AX J1832.3–0840, where the blackbody model fit is shown. For all the sources, the thin thermal plasma model (*MEKAL*; Mewe et al. 1995) gave a poor fit while the bremsstrahlung model with a partial absorption component gave an acceptable fit only for AX J1832.3–0840 with a reduced χ^2 of 1.1 for 1250 degrees of freedom. The parameters obtained from this fit are as follows : bremsstrahlung temperature, kT = $29.4^{+10.6}_{-6.9}$, interstellar absorption, $N_{\text{H}} = 0.81 \pm 0.05$ cm $^{-2}$, partial absorption, $N_{\text{H1}} = 6.2^{+0.9}_{-0.8}$ cm $^{-2}$ and the partial covering fraction = 0.68 ± 0.02 . The detection of an Fe emission lines is marked as ‘y’ in Table 4 and the further details are given in Table 5. In the case when no Fe emission line is detected, an upper limit on Fe 6.4 keV line flux is given in Table 5. This was calculated by fixing the line-center at 6.4 keV and line-width at 0.1 keV in the spectrum and fitting a Gaussian to the line. The parameters of Fe lines reported in Table 5 are measured using the power-law model fit to the spectra except for AX J1832.3–0840, for which blackbody model fit is used. Using the observed X-ray flux, we have also estimated the X-ray luminosity of our targets at a distance of 1 kpc (typical for IPs) and 8 kpc (typical for X-ray binaries) and these are listed in Table 4.

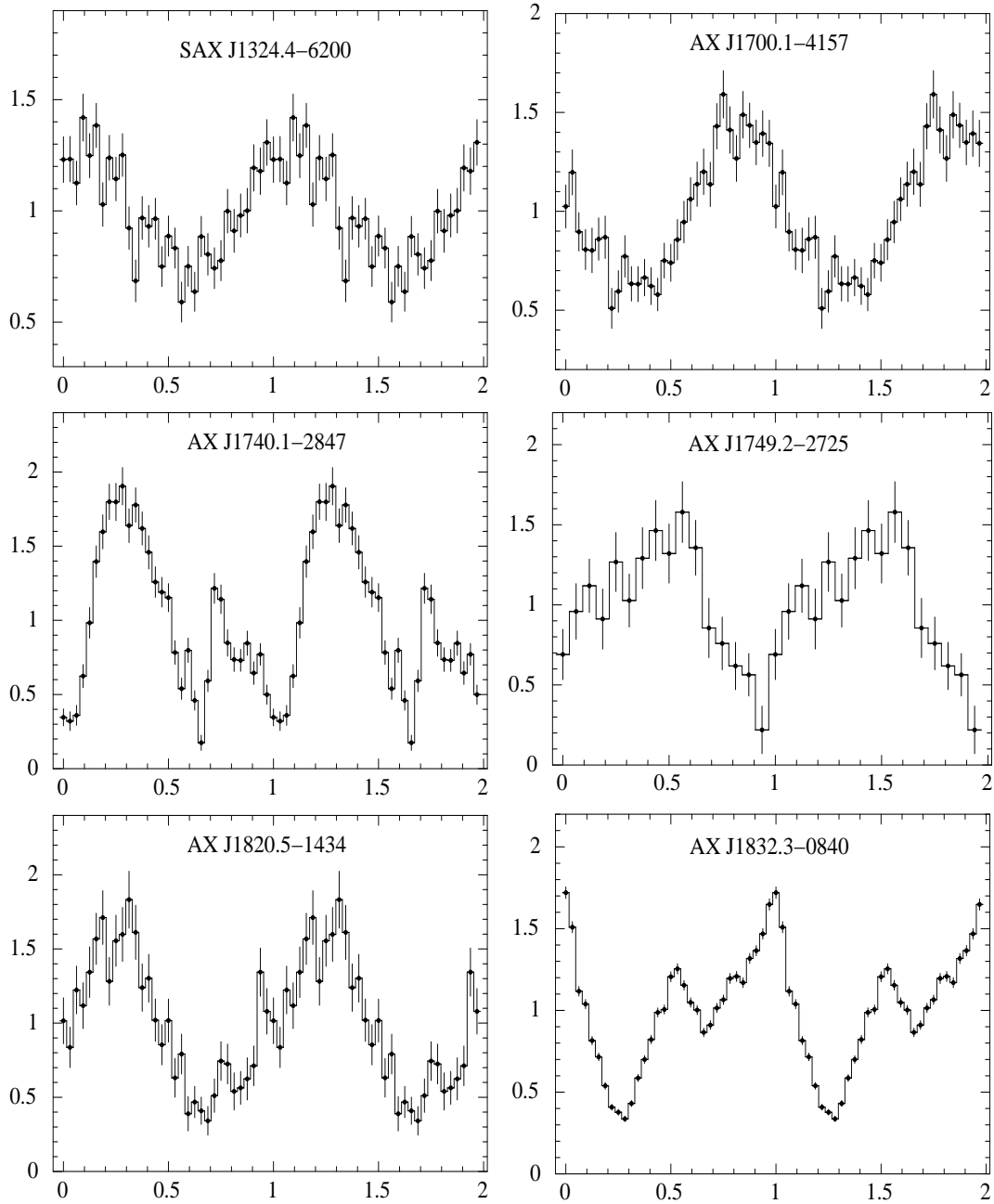


Figure 1. Pulse profiles of the X-ray pulsators from their *XMM-Newton* observations. The pulse profile of SAX J1324.4-6200 from Kaur et al. (2009) is also included for comparison.

Table 3. The pulse period, pulse fractional amplitude (%) and the spin period derivative, \dot{P} of our targets. The upper limits are quoted with 95% confidence level. SAX J1324.4-6200 is included from Kaur et al. (2009) for a comparison.

Object	Pulse period (seconds)	Pulse fractional amplitude (%)	\dot{P} ($\times 10^{-9} \text{ s s}^{-1}$)
SAX J1324.4-6200	172.57 ± 0.22	52 ± 4	6.34 ± 0.08
AX J1700.1-4157	$723.7^{+13.1}_{-1.7}$	52 ± 8	< 84
AX J1740.1-2847	$730.5^{+5.6}_{-1.0}$	81 ± 12	< 93
AX J1749.2-2725	$218.1^{+1.3}_{-1.9}$	77 ± 13	< 1
AX J1820.5-1434	153.24 ± 0.02	65 ± 11	3.00 ± 0.14
AX J1832.3-0840	$1552.3^{+2.3}_{-0.8}$	66 ± 3	< 18

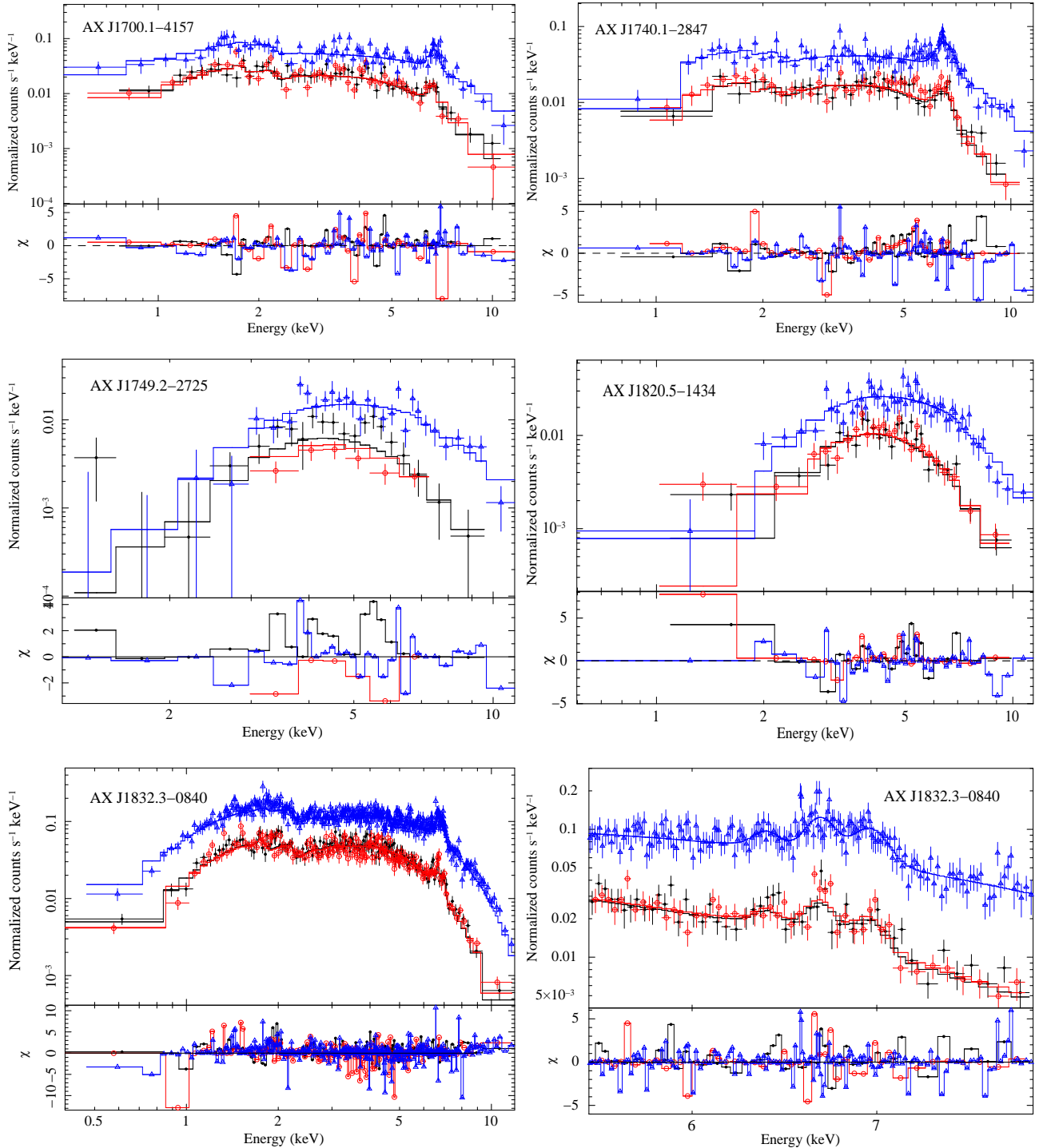


Figure 2. The *XMM-Newton* EPIC-MOS and *pn* spectra of X-ray pulsators fitted with an absorbed powerlaw model except for AX J1832.3-0840, where an absorbed blackbody model fit is shown. The EPIC-*pn*, *MOS1* and *MOS2* data points are represented by open triangles (blue color), open circles (red color) and filled circles (black color) respectively. A closer view of the X-ray spectrum of AX J1832.3-0840 from 5 - 8 keV is also provided to have a better look at different Fe emission lines.

5 INFRARED OBSERVATIONS AND DATA ANALYSIS

We retrieved near-infrared (NIR) observations of three sources - AX J1700.1-4157, AX J1740.1-2847 and AX J1749.2-2725 from the ESO - NTT archive and the details

are summarized in Table 6. These observations were made in NIR *J*, *H*, *K_s* filters with a NIR imager and spectrograph called Son-of-ISAAC (*SOFI*). The instrument was set up in large imaging mode with a pixel scale of $0''.29$ and a FOV of $5' \times 5'$ for AX J1700.1-4157 and AX J1740.1-2847, while in small imaging mode with a pixel scale of $0''.14$ and a FOV of

Table 4. The X-ray spectral parameters of our pulsators, measured using the *XMM-Newton* observations.

	AX J1700.1–4157	AX J1740.1–2847	AX J1749.2–2725	AX J1820.5–1434	AX J1832.3–0840
Power-law					
N_{H} ($\times 10^{22}$ cm $^{-2}$)	$0.52^{+0.16}_{-0.12}$	1.0 ± 0.2	$13.2^{+4.1}_{-3.5}$	$8.4^{+2.8}_{-1.0}$	0.99 ± 0.05
Γ	$0.56^{+0.13}_{-0.11}$	0.5 ± 0.1	$1.5^{+0.6}_{-0.5}$	$1.41^{+0.43}_{-0.16}$	0.83 ± 0.03
$F_{X,\text{abs}}$ ($\times 10^{-12}$ erg s $^{-1}$ cm $^{-2}$)	3.7 ± 1.2	3.4 ± 0.8	1.1 ± 1.7	1.6 ± 1.2	7.1 ± 0.5
$F_{X,\text{unabs}}$ ($\times 10^{-12}$ erg s $^{-1}$ cm $^{-2}$)	3.8 ± 1.2	3.5 ± 0.8	2.2 ± 3.0	2.5 ± 0.7	7.5 ± 0.5
Fe line	y	y	-	-	y
χ^2_{ν}/ν	1.1/245	1.0/205	1.1/55	1.0/115	1.4/1250
L_X at 1 kpc ($\times 10^{32}$ erg s $^{-1}$)	4.4 ± 1.4	4.0 ± 1.0	1.3 ± 2.0	1.9 ± 1.4	8.5 ± 0.6
L_X at 8 kpc ($\times 10^{34}$ erg s $^{-1}$)	2.8 ± 0.9	2.6 ± 0.6	0.9 ± 1.3	1.2 ± 0.9	5.4 ± 0.4
Black-body					
N_{H} ($\times 10^{22}$ cm $^{-2}$)	< 0.064	0.2 ± 0.1	$7.6^{+3.0}_{-2.3}$	$4.6^{+1.1}_{-0.9}$	0.23 ± 0.02
kT (keV)	$1.93^{+0.12}_{-0.12}$	2.4 ± 0.1	$2.1^{+0.4}_{-0.3}$	$1.92^{+0.17}_{-0.15}$	1.90 ± 0.03
$F_{X,\text{abs}}$ ($\times 10^{-12}$ erg s $^{-1}$ cm $^{-2}$)	3.3 ± 0.2	3.2 ± 0.4	1.1 ± 0.2	1.6 ± 0.1	6.8 ± 0.1
$F_{X,\text{unabs}}$ ($\times 10^{-12}$ erg s $^{-1}$ cm $^{-2}$)	3.3 ± 0.2	3.3 ± 0.4	1.5 ± 0.3	1.9 ± 0.1	6.9 ± 0.1
Fe line	y	y	-	-	y
χ^2_{ν}/ν	1.0/245	0.9/205	1.2/55	0.9/115	1.1/1250
L_X at 1 kpc ($\times 10^{32}$ erg s $^{-1}$)	3.9 ± 0.2	3.7 ± 0.5	1.3 ± 0.2	1.9 ± 0.1	8.1 ± 0.1
L_X at 8 kpc ($\times 10^{34}$ erg s $^{-1}$)	2.5 ± 0.2	2.3 ± 0.3	0.8 ± 0.2	1.2 ± 0.1	5.2 ± 0.1

Note : For all the sources, the observed fluxes ($F_{X,\text{abs}}$), unabsorbed fluxes ($F_{X,\text{unabs}}$) and the X-ray luminosities (L_X) are measured in the energy band 2 - 10 keV. The sources in which we detected the Fe emission lines are marked as ‘y’.

Table 5. Properties of the Fe emission lines detected in the X-ray spectrum of our targets using a power-law model except for AX J1832.3-0840, for which blackbody model fit is used. An upper limit on equivalent width (EW) of the Fe 6.4 keV line is given in case of non-detection of any Fe emission line in the X-ray spectrum.

Object	Fe 6.40 keV (Fluorescent)			Fe 6.67 keV (He-like)			Fe 6.97 keV (H-like)		
	Center (keV)	width (keV)	EW (eV)	Center (keV)	width (keV)	EW (eV)	Center (keV)	width (keV)	EW (eV)
AX J1700.1–4157	-	-	-	6.69 ± 0.08	0.17 ± 0.09	580	-	-	-
AX J1740.1–2847	6.5 ± 0.1	0.3 ± 0.1	998	-	-	-	-	-	-
AX J1749.2–2725	6.4 (frozen)	0.1 (frozen)	< 88	-	-	-	-	-	-
AX J1820.5–1434	6.4 (frozen)	0.1 (frozen)	< 82	-	-	-	-	-	-
AX J1832.3–0840	6.39 ± 0.03	< 0.07	50	6.67 ± 0.02	< 0.06	825	6.96 ± 0.03	0.06 ± 0.04	736

$2'.5 \times 2'.5$ for AX J1749.2–2725. During these observations, the seeing varied from $0''.6$ to $1''.0$. Images were acquired in the auto-jitter mode in which a number of single frames (NDIT) having exposure times of DIT (Detector Integrator Time) seconds were acquired at different positions and then co-averaged to generate an output image.

The data reduction is done using the standard routines in *IRAF*⁷. A master sky-frame is first constructed by median stacking all the frames of a source for each filter, which is then subtracted from all the images to generate sky-subtracted frames. These images are then flat-fielded, aligned and average stacked to obtain the final images. The astrometry and calibration of the final frames is performed using the 2MASS observations which gave an (absolute) position uncertainty of $\sim 0''.2$ for our observations.

6 IDENTIFICATION OF NIR/OPTICAL COUNTERPARTS

We searched for the near-infrared (NIR) counterparts of the X-ray sources in their ESO - NTT or 2MASS observations using the position measurement from the *Chandra* observations. The NIR K_s waveband images of our targets along with their *Chandra* images are shown in Figure 3. The black circles in this figure represent the *XMM-Newton* error circles on the position and the white circles represent the *Chandra* error circles except for AX J1820.5–1434 where the *XMM-Newton* error circle (see larger one) is also shown in white colour for clarity. As can be seen in this figure, we have very likely identified the NIR counterparts of AX J1700.1-4157, AX J1740.1-2847 and AX J1749.2-2725 in the ESO - NTT observations. For the remaining two sources - AX J1820.5-1434 and AX J1832.3-0840, a bright and a faint NIR counterpart respectively is found in the 2MASS observations. The sources identified in the 2MASS observations could be a combination of a few nearby stars which might not get resolved due to the poor resolution of the observations and therefore the probable counterparts of AX J1820.5-1434 and AX J1832.3-0840 are uncertain. The position and the J , H

⁷ IRAF is distributed by the National Optical Astronomy Observatories, USA.

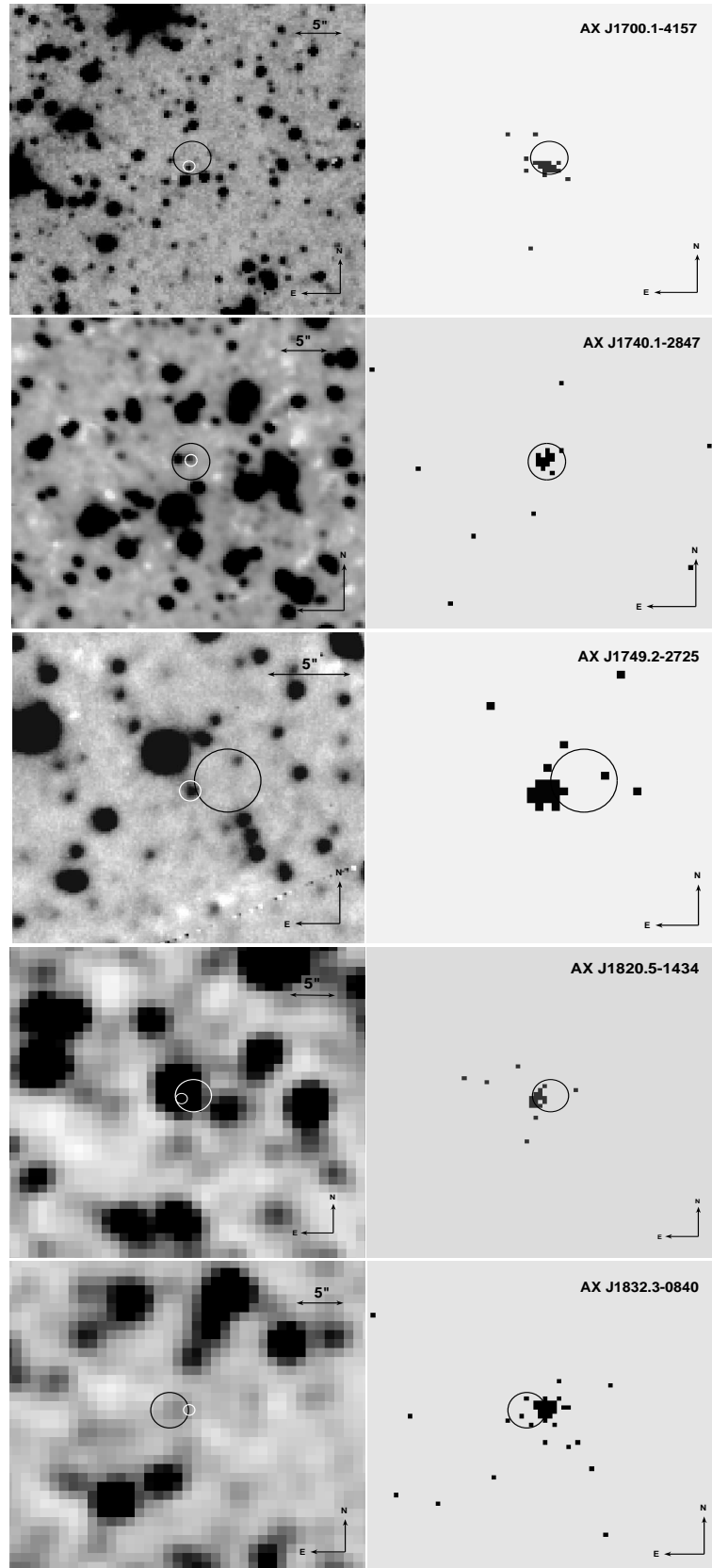


Figure 3. *Left* : The ESO-NTT NIR K_s waveband image of AX J1700.1–4157, AX J1740.1–2847, AX J1749.2–2725 and 2MASS K_s waveband image of AX J1820.5–1434 and AX J1832.2–0840. *Right* : The *Chandra* ACIS-I images of the same sources. The black and the white circles represent error circles on their position obtained from their *XMM-Newton* and the *Chandra* observations respectively, except for the NIR observations of AX J1820.5–1434 for which larger white circle represents the error circle obtained from the *XMM-Newton* observations.

Table 6. Log of the near-infrared observations obtained using 3.52-m ESO - New Technology Telescope (NTT). NDIT represents the number of single frames, having exposure times of DIT (detector integrator time) seconds and are used to generate an output image having exposure time equal to one DIT. The number of output frames are represented by Nframes.

Source	Date	Program ID	<i>J</i>			<i>H</i>			<i>K_s</i>		
			DIT	NDIT	Nframes	DIT	NDIT	Nframes	DIT	NDIT	Nframes
AX J1700.1-4157	20 Mar 2001	66.D-0440(B)	3	5	4	3	5	4	3	5	6
AX J1740.1-2847	18 Jun 2002	69.D-0339(A)	3	20	5	3	20	5	3	20	5
AX J1749.2-2725	20 Mar 2001	66.D-0440(B)	3	5	4	3	5	4	3	5	6

Table 7. The observed *J*, *H* and *K_s* magnitudes of the most likely NIR counterparts of the X-ray pulsators. The R.A. and DEC. of these sources measured from their NIR observations are also given. The position of these sources is measured with an uncertainty of $\sim 0.2''$.

Star	R.A. hh:mm:ss	DEC. ° ' "	<i>J</i> magnitude	<i>H</i> magnitude	<i>K_s</i> magnitude
AX J1700.1-4157	17:00:04.35	-41:58:05.52	17.07 ± 0.04	17.04 ± 0.05	17.38 ± 0.13
AX J1740.1-2847	17:40:09.14	-28:47:25.68	16.16 ± 0.03	15.76 ± 0.07	15.57 ± 0.10
AX J1749.2-2725	17:49:12.41	-27:25:38.25	not detected	16.89 ± 0.07	15.15 ± 0.02
AX J1820.5-1434	18:20:30.10	-14:34:22.90	15.41 ± 0.15	13.25 ± 0.07	11.75 ± 0.04
AX J1832.3-0840*	18:32:19.39	-08:40:30.53	17.11 ± 0.23	16.22 ± 0.21	16.06 ± 0.34

* - It is also detected in the Digitized Sky Survey (DSS) observations with magnitudes, R = 19.58 mag and B = 21.13 mag.

and *K_s* magnitudes of the identified sources are listed in Table 7.

We also searched for the optical counterparts of our sources in the Digitized Sky Survey (DSS)⁸ observations. For four of our sources, we identified a possible counterpart in the DSS observations while no optical counterpart is identified for AX J1820.5-1434. However, our ESO - NTT observations clearly showed that the optical counterparts found for AX J1700.1-4157, AX J1740.1-2847 and AX J1749.2-2725 are a combination of a few nearby stars, hence we do not claim detection of optical counterparts for these three sources. Out of the remaining two sources (AX J1820.5-1434 and AX J1832.3-0840) for which we did not have the ESO - NTT observations, we could only identify a possible optical counterpart for AX J1832.3-0840 in the DSS observations with magnitudes R = 19.58 mag and B = 21.13 mag, coincident with its *Chandra* position (see Figure 4). In the absence of any high-resolution observations of this source, we consider this faint optical star as its possible counterpart.

Using the neutral hydrogen column density (N_{H}) measured from the absorbed powerlaw model fit to the X-ray spectra of our targets (Table 4), we calculated the extinction towards them in the *J*, *H* and *K_s* wavebands following Predehl and Schmitt (1995) and Fitzpatrick (1999) and hence calculated the dereddened magnitudes (see Table 8). Here we assume that the companion star experiences the same N_{H} as observed for the X-ray source (i.e., no local absorption) which also allows us to put an upper limit on the extinction towards these sources.

On the basis of the extinction-free magnitudes and assuming that the sources are in our Galaxy (see Kaur et al. 2009 for the details about this method), we tentatively suggest that the NIR counterpart of AX J1700.1-4157, AX J1740.1-2847 and AX J1832.3-0840 to be a low-mass star

while of AX J1749.2-2725 to be a high mass star. The only source for which we did not have the ESO - NTT observations and which was not detected in the optical - DSS observations - AX J1820.5-1434, showed a bright NIR counterpart in the 2MASS observations. Assuming that its counterpart is a single star, we suggest it to be an early-type star. Even, using the extinction calculated from Galactic N_{H} (Dickey and Lockman 1990), this source would be compatible with an early-type star. For AX J1749.2-2725 also, a part of the N_{H} measured could be local to it, however with the Galactic N_{H} , this source remains as an early-type star with the given magnitudes.

We also found a possible tentative relation between the pulse period and the measured N_{H} of these sources. Although we have only six sources (including SAX J1324.4-6200 from Kaur et al. 2009), it seems that these sources tend to form two separate groups - having large spin period (> 700 s) and a small N_{H} ($< 10^{22}$ cm⁻²) and vice-versa, shown in Figure 5. Our analysis also showed that the sources with large pulse periods have strong Fe emission line in their spectra (shown with ‘open circles with dot inside’ in Figure 5) while the other sources did not have any signature of it (shown with ‘filled squares’ in the same figure).

7 DISCUSSION

In this paper, we aimed to find the possible counterparts of five low-luminosity X-ray pulsators and tentatively identify their nature. To achieve this goal, we obtained *Chandra* observations to measure the position of these sources with a sub-arc second accuracy which helped us to find their counterparts in the near-infrared/optical observations. We also obtained *XMM-Newton* observations of these sources to study their X-ray pulsations, pulse profiles and spectral parameters. With the help of our *XMM-Newton* observations, we have determined spin period derivative of AX J1820.5-

⁸ http://stduat.stsci.edu/cgi-bin/dss_form

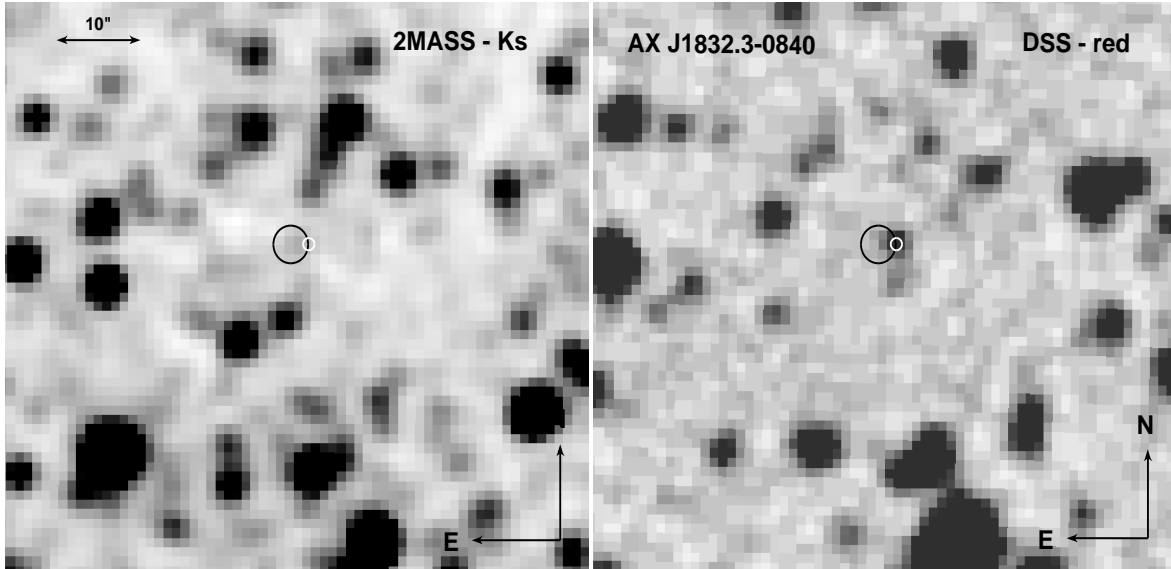


Figure 4. *Left* : 2MASS K_s waveband image of AX J1832.3–0840. *Right* : DSS image of the same source in the optical R waveband.

Table 8. Neutral hydrogen column density and the dereddened magnitudes of X-ray pulsators in J , H and K_s wavebands

Object	N_{H} ($\times 10^{22} \text{ cm}^{-2}$)	N_{H}^g ($\times 10^{22} \text{ cm}^{-2}$)	J mag	H mag	K_s mag
AX J1700.1–4157	0.5	1.8	16.26 ± 0.04	16.54 ± 0.05	17.04 ± 0.13
AX J1740.1–2847	1.1	0.9	14.45 ± 0.03	14.71 ± 0.07	14.86 ± 0.10
AX J1749.2–2725	13.2	1.5	not detected	4.25 ± 0.07	6.58 ± 0.02
AX J1820.5–1434	8.4	1.8	2.38 ± 0.15	5.21 ± 0.07	6.29 ± 0.04
AX J1832.3–0840	1.0	1.8	15.57 ± 0.23	15.27 ± 0.21	15.42 ± 0.34

NOTE : For AX J1749.2–2725 and AX J1820.5–1434, the measured N_{H} is much greater than the Galactic N_{H}^g .
 N_{H} - neutral hydrogen column density measured using powerlaw model fit to the X-ray spectrum,
 N_{H}^g - neutral hydrogen column density in the direction of the given source from Dickey and Lockman (1990)

1434 but only upper limits for the other sources. Our sources are likely neutron star binaries (with a high mass or a low mass companion) or accreting white dwarfs.

Most of the known slow X-ray pulsars are found among HMXBs except a very few which have low-mass companions. The known slow ($P_s > 0.1$ s) X-ray pulsars with low-mass companions are Her X-1, 4U 1626–67, GRO 1744–28, 4U 1822–37 and GX 1+4 (Bildsten et al. 1997, Jonker and van der Klis 2001). Four of these LMXB pulsars have spin periods between 0.5 - 10 s while only GX 1+4 has a spin-period of 140 s but also a red giant star as its companion. However, the spin period of X-ray pulsars containing high mass companions are observed upto thousands of seconds (Bildsten et al. 1997). The X-ray pulsars (both in LMXBs and HMXBs) usually display a hard X-ray spectrum well fitted with a powerlaw index, $\Gamma \sim 1.0$, or with a blackbody model of temperature, $kT \sim 2$ keV. Sometimes, their X-ray spectrum is also characterized by a strong neutral Fe emission line at 6.4 keV and very rarely ionized Fe lines at 6.7 and 6.9 keV (Ebisawa et al. 1996). These sources show both spin-up and spin-down behaviour on time-scales from a few days to a few years (Bildsten et al. 1997). The fastest spin-period derivative observed among neutron star binary pulsars is $\sim 10^{-7} \text{ s s}^{-1}$ for GX 1+4 (Elsner et al.

1985). On the other hand, intermediate polars (IPs; a subclass of white dwarf binary systems; Warner 2003) have been observed with spin periods in the range of a few hundred seconds to a few thousand seconds (Kuulkers et al. 2006). The observed X-ray spectra of most of these systems are well fitted with a thin plasma or bremsstrahlung model with temperatures of $\sim 1 - 30$ keV and characterized by strong Fe emission lines at 6.4, 6.7 and 6.9 keV (Ezuka and Ishida 1999). In most of them, the X-ray spectrum also fits well with powerlaw index, $\Gamma \leq 1.0$ (Hong et al. 2009). Most of the white dwarfs in IPs spin-up with a typical spin-period derivative of $10^{-11} \text{ s s}^{-1}$ except a few of them which spin-down. The largest spin-period derivative observed in these systems is $1.1 \times 10^{-10} \text{ s s}^{-1}$ (Mason 1997).

AX J1700.1–4157

AX J1700.1–4157, which has a pulse period of 714 s, was discovered from *ASCA* observations performed on September 16, 1997 with a hard X-ray spectrum ($\Gamma \sim 0.7$; Torii et al. 1999). It is unlikely a LMXB pulsar due to its large pulse period. The timing and spectral parameters measured from our observations are consistent with the previous observations reported by Torii et al. (1999). However, we detected a strong Fe emission line at 6.7 keV with an equivalent

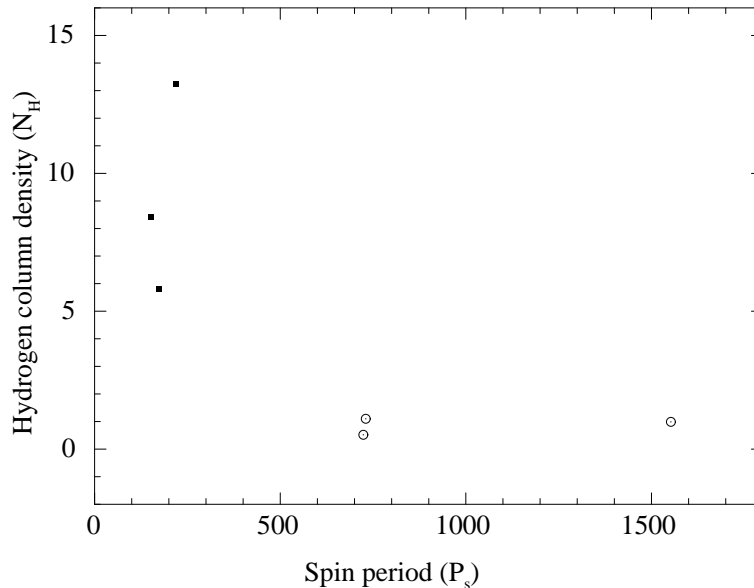


Figure 5. The spin period (P_s) versus the measured neutral hydrogen column density (N_H) of our sources. The sources represented by symbol ‘open circles with dot inside’ have Fe emission lines in their X-ray spectrum while the sources represented by symbol ‘filled square’ do not have Fe emission lines.

width of 580 eV during our observations, for which an upper limit of 1150 eV was given by Torii et al. (1999). From our NIR observations, we estimate a low mass star to be the counterpart of this source which in combination with the detection of Fe emission line would favor an IP nature of this source.

AX J1740.1–2847

AX J1740.1–2847 was discovered with a pulse period of 729 ± 14 s from observations performed on September 7 - 8, 1998 using *ASCA* and with a hard X-ray spectrum ($\Gamma \sim 0.7$; Sakano et al. 2000). The large pulse period of this source makes it unlikely to be a LMXB pulsar. The timing and spectral parameters measured from our observations are consistent with the previous measurement except that we detected a strong Fe 6.4 keV line in the X-ray spectrum with an equivalent width of 998 eV which was not detected during the *ASCA* observations and an upper limit of 500 eV was given on its equivalent width (Sakano et al. 2000). With the given NIR magnitudes, we suggest a low mass star to be the possible counterpart of this source, favoring an IP interpretation.

AX J1749.2–2725

AX J1749.2–2725, discovered with a pulse period of 220.38 ± 0.20 s during the *ASCA* observations performed on March 26, 1995, was detected with the X-ray spectrum having powerlaw index of 1.0 (Torii et al. 1998). During our observations, AX J1749.2–2725 was detected with similar timing and spectral parameters as were reported by Torii et al. (1998). No Fe emission line was detected in the X-ray spectrum during the previous as well as the present observations. From our NIR observations, we infer a high mass star as a possible counterpart which favors a HMXB pulsar nature for this source.

AX J1820.5–1434

AX J1820.5–1434 was detected with a pulse period of

152.26 ± 0.04 s from the *ASCA* observations made on April 8 - 12, 1997 and with a hard X-ray spectrum ($\Gamma \sim 0.9$; Kinugasa et al. 1998). The observed timing and spectral parameters from our observations are consistent with those reported by Kinugasa et al. (1998). The accurate spin-period measurement from our observations, in combination with the previous spin-period measurement (Table 1) resulted in a spin-period derivative determination of this source of $(3.00 \pm 0.14) \times 10^{-9}$ s s $^{-1}$. The largest spin-period derivative measured in IPs is 1.1×10^{-10} s s $^{-1}$ (Mason 1997). Thus, this source is unlikely a white dwarf system. Although we identified a bright NIR counterpart of this source in the 2MASS observations, we caution against drawing any conclusions on the basis of it since it could be a combination of a few nearby stars overlapped. The high spin-down rate of this source favors a neutron star nature, but we cannot distinguish between a low mass or a high mass X-ray binary.

AX J1832.3–0840

AX J1832.3–0840 which has a pulse period of 1550 s, was discovered during observations performed on October 11, 1997 using *ASCA*, with a hard X-ray spectrum ($\Gamma \sim 0.8$; Sugizaki et al. 2000). During these observations, a strong 6.7 keV Fe emission line was detected in the X-ray spectrum and the spectrum was also satisfactorily fitted with a thermal-equilibrium plasma model (Raymond and Smith 1977). During our observations, we measured the similar timing and the spectral parameters with respect to the previous observations. However, we detected three Fe emission lines in the X-ray spectrum of this source (see Figure 2), which are typically seen in IPs. Our X-ray spectrum satisfactorily fitted with a bremsstrahlung model of temperature ~ 30 keV, which is common among IPs and is rare among X-ray pulsars. We identified a faint counterpart of this source in the DSS as well as 2MASS observations, which indicate a low-mass star as its counterpart. Therefore, we suggest this source to be likely an IP.

8 CONCLUSIONS

Our multiwavelength observations have helped us to identify the very likely near-infrared/optical counterparts for most of our targets. The X-ray flux of all the sources is found consistent with their previous measurements and the non-detection of any period of quiescence in them confirmed their persistent nature. The pulse profiles and pulse fractional amplitudes from our observations are found to be consistent with the previous observations, indicating that these are stable systems. Our observations also suggest that these sources might form two different groups - with large pulse period having small N_H and detection of Fe lines and small pulse period having large N_H and non-detection of any Fe emission line (Figure 5). With the help of our multiwavelength observations, we suggest AX J1749.2-2725 and AX J1820.5-1434 to be accreting neutron star systems while the remaining three sources could be IPs. The NIR spectroscopic observations of these sources would help us to find the exact nature of the counterparts and to unveil their true nature.

REFERENCES

- Aldcroft T.L., Karovska M., Cresitello-Dittmar M.L., Cameron R.A. and Markevitch M.L. 2000, in Truemper J.E. and Aschenbach B., eds, Proc. SPIE Vol. 4012, *X-ray Optics, Instruments, and Missions III*. SPIE, Bellingham, p. 650
- Bildsten L., Chakrabarty D., Chiu J. et al. 1997, ApJS, 113, 367
- Dickey J.M. and Lockman F.J. 1990, ARA&A, 28, 215
- Ebisawa K., Day C.S.R., Kallman T.R. et al. 1996, PASJ, 48, 425
- Elsner R.F., Weisskopf M.C., Apparao K.M.V. et al. 1985, ApJ, 297, 288
- Ezuka H. and Ishida M. 1999, ApJS, 120, 277
- Fitzpatrick E.L. 1999, PASP, 111, 63
- Hong J.S., van den Berg M., Laycock S., Grindlay J.E. and Zhao P. 2009, ApJ, 699, 1053
- Hulleman F., in 't Zand J.J.M. and Heise J. 1998, A&A, 337, L25
- Jonker P.G. and van der Klis M. 2001, ApJ, 553, L43
- Kaur R., Wijnands R., Patruno A. et al. 2009, MNRAS, 394, 1597
- Kinugasa K., Torii K., Hashimoto Y. et al. 1998, ApJ, 495, 435
- Kuulkers E., Norton A., Schwope A. and Warner B. 2006, in Compact stellar X-ray sources, ed. W. H. G. Lewin & M. van der Klis (Cambridge: Cambridge Univ. Press), 421
- Lin X.B., Church M.J., Nagase F. and Bałucińska-Church M. 2002, MNRAS, 337, 1245
- Makishima K. in Mason, K. O., Watson, M. G., & White, N. E. eds, *The Physics of Accretion onto Compact Objects* Springer-Verlag, Berlin, p. 249
- Mason K.O. 1997, MNRAS, 285, 493
- Mewe R., Kaastra J.S., Schrijver C.J., van den Oord G.H.J. and Alkemade F.J.M. 1995, A&A, 296, 477
- Misaki K., Terashima Y., Kamata Y. et al. 1996, ApJL, 470, L53
- Okazaki A.T. and Negueruela I. 2001, A&A, 377, 161
- Pfahl E., Rappaport S., Podsiadlowski P. and Spruit H. 2002, ApJ, 574, 364
- Predehl P. and Schmitt J.H.M.M. 1995, A&A, 293, 889
- Raymond J.C. and Smith B.W. 1977, ApJS, 35, 419
- Reig P. and Roche P. 1999, MNRAS, 306, 100
- Sakano M., Torii K., Koyama K., Maeda Y. and Yamauchi S. 2000, PASJ, 52, 1141
- Strüder L., Briel U., Dennerl K. et al. 2001, A&A, 365, L18
- Sugizaki M., Kinugasa K., Matsuzaki K. et al. 2000, ApJL, 534, L181
- Sugizaki M., Mitsuda K., Kaneda H. et al. 2001, ApJS, 134, 77
- Torii K., Kinugasa K., Katayama K. et al. 1998, ApJ, 508, 854
- Torii K., Sugizaki M., Kohmura T., Endo T. and Nagase F. 1999, ApJL, 523, L65
- Turner M.J.L., Abbey A., Arnaud M. et al. 2001, A&A, 365, L27
- van den Berg M., Tagliaferri G., Belloni T. and Verbunt F. 2004, A&A, 418, 509
- Warner B. 2003, *Cataclysmic Variable Stars*. Cambridge Univ. Press, Cambridge